

## Polymer-Controlled Synthesis of Silver Nanobelts and Hierarchical Nanocolumns

Jingwei Bai, Yao Qin, Chengyang Jiang, and Limin Qi\*

Beijing National Laboratory for Molecular Sciences, State Key Laboratory for Structural Chemistry of Unstable and Stable Species, College of Chemistry, Peking University, Beijing 100871, P. R. China

Received March 22, 2007

Revised Manuscript Received May 29, 2007

One-dimensional (1D) metal nanostructures have received extensive attention because of their unique electrical, optical, thermal, and mechanical properties and the potential applications in electronics, photonics, (bio)chemical sensing and imaging, catalysis, etc.<sup>1</sup> Among the metals, 1D silver nanostructures are especially attractive because bulk silver exhibits the highest electrical and thermal conductivities, and nanoscale silver displays strong surface plasmon resonance largely dependent on its size and shape.<sup>2</sup> The solution-phase synthesis involving capping agents such as surfactants, polymers, and certain ionic species has proven to be very effective in the controlled synthesis of 1D silver nanostructures; notable examples include the seed-mediated synthesis in aqueous solutions of cetyltrimethylammonium bromide (CTAB)<sup>3</sup> and the polyol synthesis in the presence of poly(vinyl pyrrolidone) (PVP).<sup>4</sup> There are continued efforts devoted to the facile or rapid solution synthesis of silver nanorods and nanowires.<sup>5–7</sup> On the other hand, considerable attention has been paid to the shape-controlled synthesis of 1D silver nanostructures. For example, silver nanobeams<sup>8</sup> with interesting electrical properties and silver nanobars and nanorices<sup>9</sup> showing novel optical properties were prepared through modified polyol synthesis recently. It is noteworthy that unique silver nanobelts coexisting with silver nanoplates were fabricated by refluxing an aqueous silver colloidal

dispersion; however, the yield of the nanobelts was quite low (~5%) and the nanobelts was very thin and thus tended to break into segments.<sup>10</sup> It remains a great challenge to realize the high-yield production of silver nanobelts with good mechanical stability. Moreover, it would be highly desirable to fabricate 1D silver nanostructures with hierarchical architectures in solution because architectural manipulation of 1D silver nanostructures could further endow them with unique properties and promising applications.

Recently, polymer-directed crystallization has been widely used for the biomimetic or bioinspired synthesis of inorganic nanostructures with controlled shapes and complex architectures.<sup>11</sup> A variety of synthetic hydrophilic polymers have been employed as effective structure-directing agents in aqueous-phase synthesis.<sup>12</sup> Specifically, double-hydrophilic block copolymers turned out to be powerful in controlling inorganic crystallization,<sup>13</sup> whereas some commercial homopolymers such as poly(acrylic acid) (PAA) played key roles in the formation of elegant inorganic superstructures.<sup>14</sup> Nevertheless, there are only limited reports on the polymer-directed synthesis of 1D metal nanostructures in aqueous solutions.<sup>6</sup> Herein, we report a facile low-temperature synthesis of unique silver nanobelts as well as hierarchical nanocolumns consisting of stacked silver nanoplates under the direction of PAA in aqueous solutions.

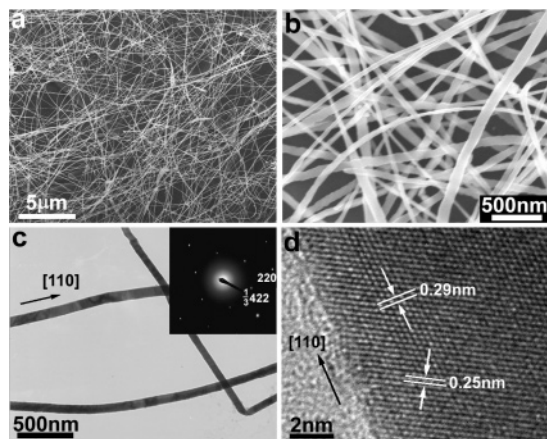
Silver nanobelts were readily synthesized by reducing AgNO<sub>3</sub> with ascorbic acid in aqueous solutions of PAA ( $M_w = 2100$ , sodium salt, Aldrich) at 4 °C; for the synthesis of silver hierarchical nanocolumns, acetic acid (HAc) was introduced with the synthesis procedure essentially unchanged (see the Supporting Information). The products were characterized by scanning electron microscopy (SEM, Hitachi S4800, 10 kV), transmission electron microscopy (TEM, JEOL JEM-200CX, 160 kV), high-resolution TEM (HR-TEM, FEI Tecnai F30, 300 kV), X-ray diffraction (XRD, Rigaku Dmax-2000).

Figure 1a presents a representative low-magnification SEM image of the silver product obtained at a PAA concentration of 1.6 mg L<sup>-1</sup>, which apparently consists of wrapped nanofibers up to several tens of micrometers in length. The XRD pattern of these nanobelts (see the Supporting Information, Figure S1) exhibits reflections characteristic of the cubic Ag (JCPDS 04-0783), indicating that the nanobelts are composed of pure silver. A high-magnification SEM image shown in Figure 1b clearly shows that the wirelike nanostructures are actually silver nanobelts typically ranging from 60 to 100 nm in width and about 30–40 nm in thickness. A

\* Corresponding author. E-mail: liminqi@pku.edu.cn

- (1) (a) Chen, J.; Wiley, B. J.; Xia, Y. *Langmuir* **2007**, *23*, 4120. (b) Murphy, C. J.; Sau, T. K.; Gole, A. M.; Orendorff, C. J.; Gao, J.; Gou, L.; Hunyadi, S. E.; Li, T. *J. Phys. Chem. B* **2005**, *109*, 13857. (c) Murphy, C. J.; Gole, A. M.; Hungyadi, S. E.; Orendorff, C. J. *Inorg. Chem.* **2006**, *45*, 7544.
- (2) Wiley, B. J.; Im, S. H.; Li, Z.-Y.; McLellan, J.; Siekkinen, A.; Xia, Y. *J. Phys. Chem. B* **2006**, *110*, 15666.
- (3) (a) Jana, N. R.; Gearheart, L.; Murphy, C. J. *Chem. Commun.* **2001**, 617. (b) Murphy, C. J.; Jana, N. R. *Adv. Mater.* **2002**, *14*, 80.
- (4) (a) Sun, Y.; Gates, B.; Mayers, B.; Xia, Y. *Nano Lett.* **2002**, *2*, 165. (b) Sun, Y.; Yin, Y.; Mayers, B. T.; Herricks, T.; Xia, Y. *Chem. Mater.* **2002**, *14*, 4736. (c) Sun, Y.; Mayers, B.; Herricks, T.; Xia, Y. *Nano Lett.* **2003**, *3*, 955.
- (5) (a) Caswell, K. K.; Bender, C. M.; Murphy, C. J. *Nano Lett.* **2003**, *3*, 667. (b) Hu, J.-Q.; Chen, Q.; Xie, Z.-X.; Han, G.-B.; Wang, R.-H.; Ren, B.; Zhang, Y.; Yang, Z.-L.; Tian, Z.-Q. *Adv. Funct. Mater.* **2004**, *14*, 183.
- (6) Zhang, D.; Qi, L.; Yang, J.; Ma, J.; Cheng, H.; Huang, L. *Chem. Mater.* **2004**, *16*, 872.
- (7) (a) Gou, L.; Chipara, M.; Zaleski, J. M. *Chem. Mater.* **2007**, *19*, 1755. (b) Tsuji, M.; Matsumoto, K.; Miyamae, N.; Tsuji, T.; Zhang, X. *Cryst. Growth Des.* **2007**, *7*, 311.
- (8) Wiley, B. J.; Wang, Z.; Wei, J.; Yin, Y.; Cobden, D. H.; Xia, Y. *Nano Lett.* **2006**, *6*, 2273.
- (9) Wiley, B.; Chen, Y.; McLellan, J.; Xiong, Y.; Li, Z.-Y.; Ginger, D.; Xia, Y. *Nano Lett.* **2007**, *7*, 1032.

- (10) Sun, Y.; Mayers, B.; Xia, Y. *Nano Lett.* **2003**, *3*, 675.
- (11) (a) Xu, A.-W.; Ma, Y.; Cölfen, H. *J. Mater. Chem.* **2007**, *17*, 415. (b) Cölfen, H.; Yu, S.-H. *MRS Bull.* **2005**, *30*, 727. (c) Cölfen, H.; Antonietti, M. *Angew. Chem., Int. Ed.* **2005**, *44*, 5576.
- (12) Yu, S.-H.; Cölfen, H. *J. Mater. Chem.* **2004**, *14*, 2124.
- (13) (a) Qi, L.; Cölfen, H.; Antonietti, M. *Angew. Chem., Int. Ed.* **2000**, *39*, 604. (b) Yu, S.-H.; Cölfen, H.; Tauer, K.; Antonietti, M. *Nat. Mater.* **2005**, *4*, 51.
- (14) (a) Yu, S.-H.; Antonietti, M.; Cölfen, H.; Hartmann, J. *Nano Lett.* **2003**, *3*, 379. (b) Oaki, Y.; Imai, H. *Angew. Chem., Int. Ed.* **2004**, *43*, 1363.



**Figure 1.** (a, b) SEM, (c) TEM, and (d) HRTEM images of silver nanobelts obtained at  $[PAA] = 1.6 \text{ mg L}^{-1}$ . Inset shows the ED pattern corresponding to the nanobelt located at the upper-left corner.

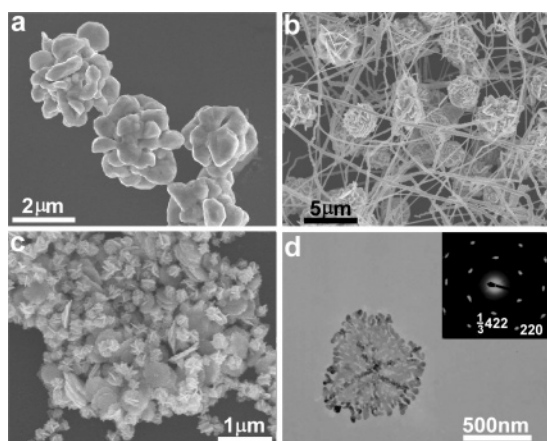


**Figure 2.** (a–c) SEM and (d) TEM images of silver products obtained at different PAA concentrations. Inset shows the corresponding ED pattern.  $[PAA]$ : (a) 0, (b) 0.5, and (c, d)  $160 \text{ mg L}^{-1}$ .

typical TEM image of the silver nanobelts is presented in Figure 1c, which shows the twisting of a nanobelt, confirming the beltlike structure. The selected area electron diffraction (ED) pattern of an individual nanobelt can be indexed to the  $[111]$  zone axis of cubic silver, indicating that the Ag nanobelt is a single crystal grown along the  $[110]$  direction and enclosed by the  $\{111\}$  and  $\{211\}$  planes as the top and side surfaces, respectively. The appearance of weak spots corresponding to the forbidden  $(1/3)\{422\}$  reflection suggests that the facets parallel to the TEM grid are smooth and flat.<sup>10</sup> The HRTEM image of an individual Ag nanobelt is shown in Figure 1d, which exhibits clear fringes with a spacing of 0.25 nm responsible for the  $(1/3)\{422\}$  reflection and a spacing of 0.29 nm due to the  $(110)$  reflection, confirming that each Ag nanobelt is a  $[110]$ -oriented single crystal. Compared with the thin silver nanobelts ( $\sim 9$  nm in diameter) previously obtained with a yield of  $\sim 5\%$  by refluxing a colloidal Ag dispersion,<sup>10</sup> the current Ag nanobelts showing the same growth direction have a yield near 100% and are relatively thicker (30–50 nm) and wider (60–100 nm) with a much better mechanical stability.

The synthesis was also carried out at different PAA concentrations under otherwise identical conditions to elucidate the effect of PAA. As shown in Figure 2a, micrometer-sized silver particles showing irregular protrusions were

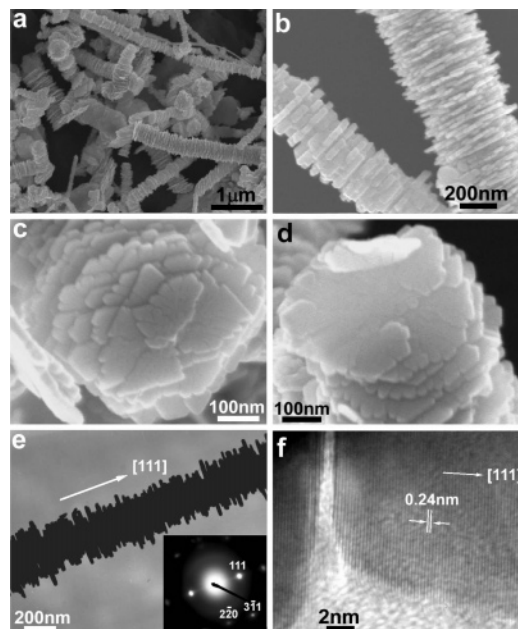


**Figure 3.** (a–d) SEM, (e) TEM, and (f) HRTEM images of silver nanocolumns obtained in the presence of HAc. Inset shows the corresponding ED pattern.

obtained in the absence of PAA. In the presence of  $0.5 \text{ mg L}^{-1}$  PAA, some silver nanobelts were obtained in addition to the silver microparticles (Figure 2b). Pure silver nanobelts would be produced at a PAA concentration of  $1.6 \text{ mg L}^{-1}$  as shown in Figure 1. If the PAA concentration was further increased to  $160 \text{ mg L}^{-1}$ , submicrometer-sized branched particles consisting of silver nanoplates about 20–30 nm in thickness were obtained (Figure 2c). The TEM image of a single nanoplate as well as its ED pattern suggested that each nanoplate was a  $[111]$ -oriented single crystal (Figure 2d). These results indicated that PAA could strongly adsorb on the  $\{111\}$  planes of silver and less strongly adsorb on the  $\{211\}$  planes at a medium PAA concentration (e.g.,  $1.6 \text{ mg L}^{-1}$ ), leading to the formation of the  $[110]$ -oriented silver nanobelts with the top surface of the  $\{111\}$  plane. At a lower PAA concentration, the capping effect of PAA was less-pronounced so that a mixture of silver nanobelts and microparticles were produced. At a much higher PAA concentration, the adsorption of the polymer on the planes other than the  $\{111\}$  and  $\{211\}$  planes would become pronounced and comparable to its adsorption on the  $\{211\}$  planes, leading to the formation of the silver particles consisting of  $[111]$ -oriented nanoplates.

Interestingly, unusual hierarchical silver nanocolumns consisting of stacked nanoplates can be produced as precipitates at the bottom of the glass tube rather than thin films on the glass wall when acetic acid was introduced into the reaction solution with suitable PAA and reactant concentrations (Figure 3). As shown in Figure 3a, many silver nanocolumns typically 300–500 nm in diameter, which looked like “stacks of pancakes”, were obtained together with some nanoplates and nanobelts. A high-magnification SEM image shown in Figure 3b suggests that the nanocolumns actually consist of face-to-face stacked nanoplates with a thickness about 20–40 nm. Close observations on the end faces of the nanocolumns show that the growth steps did

not show a helical pattern, in contrast to the observation from helical ZnO nanocolumns grown from solution<sup>15</sup> and stacked calcite superstructures obtained from microemulsions.<sup>16</sup> Figure 3e shows a typical TEM image of a single silver nanocolumn together with its ED pattern, which indicates that the nanocolumn is a single crystal grown along the [111] direction and all the face-to-face stacked nanoplates are [111]-oriented. The HRTEM image presented in Figure 3f shows clear lattice fringes with a  $d$  spacing of  $\sim 0.24$  nm corresponding to the silver (111) plane from neighboring nanoplates, confirming that the whole stack of pancakes are actually [111]-oriented single-crystalline silver nanocolumns. The obtained hierarchical silver nanocolumns are reminiscent of the stacks of pancakes reported for  $\text{CaCO}_3$ ,<sup>16</sup>  $\text{ZnO}$ ,<sup>17,18</sup> and  $\text{Ni}(\text{OH})_2$ .<sup>19</sup> Nevertheless, to the best of our knowledge, this is the first time that such an architecture has been chemically synthesized for metals. The silver nanocolumns showing parallel nanoplates extending perpendicular to the stem may find promising applications in surface-enhanced Raman scattering (SERS) detection.<sup>20</sup>

Basically, there are three possible growth mechanism for the silver nanocolumns made of stacked nanoplates, i.e., face-to-face assembly of preformed individual silver nanoplates, growth of nanoplates perpendicularly on the preformed central stem, and step-by-step growth of additional nanoplates on the top surface of preformed nanoplates or nanocolumns. It was observed that the nanocolumns could usually withstand significant levels of physical stress such as strong ultrasonic treatment; moreover, after being dissolved in 3 M  $\text{HNO}_3$  solution for a short time (approximately several seconds), the nanocolumns became coarse stems without obvious platelike subunits, which were still single crystals elongated along the [111] direction (see the Supporting Information, Figure S2). These results indicated that the lamellae were held together by the single-crystalline inner stem to construct the final nanocolumns, thus excluding the possibility of assembly of preformed discrete silver nanoplates. To distinguish the other two possible growth mechanisms, the time-dependent growth process for the nanocolumns were investigated preliminarily. At a very short reaction time (e.g., less than 4 h), some nanocolumns consisting of stacked nanoplates were produced, together with some nanoplates and nanobelts, but [111]-oriented nanorods with relatively smooth surfaces could not be observed. This result strongly indicated that the hierarchical silver nanocolumns were formed by step-by-step growth of additional nanoplates on the top surface

of preformed nanoplates or nanocolumns, i.e., the stacks developed by gradual propagation of surface steps from a primary [111]-oriented single-crystalline nanoplate.

It remains unclear why the presence of HAc considerably favored the stacking of silver nanoplates to form hierarchical nanocolumns. The pH of the initial reaction solution was measured to be 3.6, which was lower than the  $\text{p}K_a$  of the PAA ( $\sim 4.3$ ),<sup>21</sup> indicating that the PAA molecules were partially protonated and somewhat hydrophobic. It is known that the protonation of the PAA molecules could affect the adsorption of PAA on silver surfaces and the acetic ions themselves could also participate in capping silver surfaces, implying a cooperative effect of PAA and HAc in the formation of the silver nanocolumns. In the current situation, the {111} planes could still be the most stable planes because of the strong specific adsorption of PAA, favoring the formation of [111]-oriented silver plates. Meanwhile, the central part of the top surface of the nanoplates could adsorb fewer capping ions such as the  $\text{Ac}^-$  ions during the growth process because the capping molecules would reach the outer part of the surface with a more probability. The central part of the surface would show a higher growth tendency, leading to the growth of another nanoplate from the central part of the top surface of the primary nanoplate and finally to the formation of nanocolumns made by stacked nanoplates. It is noteworthy that the HAc may be substituted with some other organic acids for the formation of the nanocolumns; specifically, silver nanocolumns with a relatively low yield were also obtained when excess ascorbic acid was present in place of HAc.

In conclusion, [110]-oriented single-crystalline silver nanobelts larger than  $10 \mu\text{m}$  in length, 60–100 nm in width, and 30–40 nm in thickness were synthesized readily in aqueous solutions under the direction of poly(acrylic acid) at 4 °C. Moreover, unique hierarchical silver nanocolumns consisting of stacked nanoplates were fabricated in aqueous poly(acrylic acid) solutions in the presence of acetic acid. The obtained silver nanobelts show good mechanical stability and could be an ideal candidate for investigating the electrical properties of 1D metal nanostructures with a specific cross-sectional aspect ratio,<sup>22</sup> whereas the silver nanocolumns could find promising applications in SERS detection. This synthetic strategy based on polymer-directed crystallization in aqueous solutions may open a new route for the green, high-yield synthesis of metal nanobelts and the controllable fabrication of hierarchical metal architectures.

**Acknowledgment.** This work was supported by NSFC (20325312, 20673007, 20473003, 20633010, and 50521201) and the President Grant of Peking University.

**Supporting Information Available:** Detailed synthesis procedure, XRD pattern of Ag nanobelts, and EM images of partially dissolved Ag nanocolumns (PDF). This material is available free of charge via the Internet at <http://pubs.acs.org>.

CM0707861

- (15) Tian, Z. R.; Voigt, J. A.; Liu, J.; McKenzie, B.; McDermott, M. J. *J. Am. Chem. Soc.* **2002**, *124*, 12954.
- (16) Viravaidya, C.; Li, M.; Mann, S. *Chem. Commun.* **2004**, 2182.
- (17) Tian, Z. R.; Voigt, J. A.; Liu, J.; McKenzie, B.; McDermott, M. J.; Rodriguez, M. A.; Konishi, H.; Xu, H. *Nat. Mater.* **2003**, *2*, 821.
- (18) Taubert, A.; Kulbel, C.; Martin, D. C. *J. Phys. Chem. B* **2003**, *107*, 2660.
- (19) Coudun, C.; Hochepeid, J.-F. *J. Phys. Chem. B* **2005**, *109*, 6069.
- (20) Tao, A.; Kim, F.; Hess, C.; Goldberger, J.; He, R.; Sun, Y.; Xia, Y.; Yang, P. *Nano Lett.* **2003**, *3*, 1229.
- (21) Wang, Y.; Caruso, F. *Chem. Mater.* **2006**, *18*, 4089.
- (22) Wiley, B. J.; Wang, Z.; Wei, J.; Yin, Y.; Cobden, D. H.; Xia, Y. *Nano Lett.* **2006**, *6*, 2273.